Journal of Cardiovascular Computed Tomography xxx (xxxx) xxx

Contents lists available at ScienceDirect

Journal of Cardiovascular Computed Tomography

journal homepage: www.JournalofCardiovascularCT.com

Review Article

Myocardial late enhancement and extracellular volume with single-energy, dual-energy, and photon-counting computed tomography

Noriko Oyama-Manabe [a], Seitaro Oda [b], Yasutoshi Ohta [c], Hidenobu Takagi [d,e], Kakuya Kitagawa [f,*], Masahiro Jinzaki [g]

[a] Department of Radiology, Jichi Medical University Saitama Medical Center, Saitama, Japan
[b] Department of Diagnostic Radiology, Faculty of Life Sciences, Kumamoto University, Kumamoto, Japan
[c] Department of Radiology, National Cerebral and Cardiovascular Center, Suita, Japan
[d] Department of Advanced Radiological Imaging Collaborative Research, Tohoku University, Sendai, Japan
[e] Department of Diagnostic Radiology, Tohoku University Hospital, Sendai, Japan
[f] Department of Radiology, Mie University Hospital, Tsu, Japan
[g] Department of Radiology, Keio University, Shinjuku-ku, Japan

ARTICLE INFO

Keywords:
Computed tomography
Late enhancement
Extracellular volume
Dual-energy CT
Photon-counting detector CT

ABSTRACT

Computed tomography late enhancement (CT-LE) is emerging as a non-invasive technique for cardiac diagnosis with wider accessibility compared to MRI, despite its typically lower contrast-to-noise ratio. Optimizing CT-LE image quality necessitates a thorough methodology addressing contrast administration, timing, and radiation dose, alongside a robust understanding of extracellular volume (ECV) quantification methods. This review summarizes CT-LE protocols, clinical utility, and advances in ECV measurement through both single-energy and dual-energy CT. It also highlights photon-counting detector CT technology as an innovative means to potentially improve image quality and reduce radiation exposure.

1. Introduction

Late gadolinium enhancement (LGE) magnetic resonance imaging (MRI) has been widely used as a non-invasive reference standard for myocardial infarction and focal fibrosis.[1,2] A firm grasp of the distribution pattern of LGE aids in differentiating ischemic cardiomyopathies from non-ischemic cardiomyopathies.[3] Di Marco et al. reported that the presence of LGE indicates a high risk of developing ventricular arrhythmias and sudden death even in patients with NYHA class I non-ischemic cardiomyopathy.[4] Thus, the presence of LGE is an independent predictor of the prognosis of various cardiac diseases.[5] Looking back at the history of delayed contrast enhancement in CT, reports of iodine contrast effects on myocardial infarction in animal experiments through CT can be traced back to the 1980s.[6] Subsequently, there have also been reports of myocardial infarction assessments using CT imaging following invasive cardiac catheterization procedures.[7] The usefulness of myocardial computed tomography late enhancement (CT-LE) for detecting ischemic heart disease and various non-ischemic myocardial diseases has been reported.[8–10] CT is an attractive alternative to cardiac MRI, particularly in cases where MRI is contraindicated.[11] CT can be a comprehensive examination for detecting ischemic and non-ischemic cardiomyopathies with combined coronary CT angiography (CCTA) and CT-LE protocol as non-ischemic cardiomyopathy could be evaluated with the CT-LE after excluding the diagnosis of coronary artery disease. Compared with that of MRI, the diagnostic accuracy of CT for detecting late enhancement (LE) in ischemic and non-ischemic patterns is high.[12] CT-LE is observed in about one-thirds of patients undergoing CCTA for suspected ischemic heart disease.[13] Multivariate analysis has shown that CT-LE positivity was higher in men and patients with a history of heart failure hospitalization.[13]

Goto et al. reported that in addition to common clinical risk factors and CCTA findings, the presence of CT-LE is an independent predictor of major adverse cardiovascular event (MACE) in patients with suspected coronary artery disease. CT-LE imaging performed after CCTA could help identify high-risk patients with suspected coronary artery disease who

Abbreviations: CCTA, coronary computed tomography angiography; CI, confidence interval; CNR, contrast-to-noise ratio; CT, computed tomography; CT-LE, computed tomography late enhancement; ECV, extracellular volume; LE, late enhancement; LGE, late gadolinium enhancement; MRI, magnetic resonance imaging; PCD, photon counting detector; VMI, virtual mono-energetic image.

* Corresponding author. Department of Radiology, Mie University Hospital, 2-174 Edobashi, Tsu, Mie, 514-8507, Japan.
E-mail address: kakuya@med.mie-u.ac.jp (K. Kitagawa).

https://doi.org/10.1016/j.jcct.2023.12.006
Received 27 September 2023; Received in revised form 16 November 2023; Accepted 14 December 2023
Available online xxxx

Please cite this article as: Oyama-Manabe N et al., Myocardial late enhancement and extracellular volume with single-energy, dual-energy, and photon-counting computed tomography, Journal of Cardiovascular Computed Tomography, https://doi.org/10.1016/j.jcct.2023.12.006

may benefit from more intensive medical or revascularization therapies.[14] LGE may not be able to detect diffuse fibrosis; however, extracellular volume (ECV) measured via cardiac magnetic resonance T1-mapping can be used to quantify diffuse myocardial damage caused by various cardiac diseases.[15,16] CT-LE can also be employed for the calculation of ECV. A recent systemic review and meta-analysis demonstrated that CT-derived ECV showed excellent correlation with MRI-derived ECV.[17] This review article provides an overview of the standard CT-LE imaging protocol and tips for enhancing the efficacy of CT-LE, as well as the clinical utility of CT-LE and ECV measurements.

2. Technique and tips to acquire high-quality CT-LE images

2.1. Acquisition and reconstruction of CT-LE

CT-LE is defined as delayed imaging after the injection of a contrast medium to evaluate for delayed enhancement of the myocardium.[18] The imaging parameters should be optimized to enhance myocardial contrast, as the contrast between the remote and hyper-enhanced myocardium is much lower in CT-LE than that in LGE-MRI.[19] Low tube potential imaging at 70 or 80 kVp is an effective approach for CT-LE as it permits radiation dose reduction and augmented contrast enhancement. The usefulness of iterative reconstruction,[20–22] deep learning reconstruction,[23] and image averaging[24] has been demonstrated against the increase in image noise associated with the use of low tube potentials. Use of low-contrast targeted image reconstruction is recommended compared with high-contrast targeted image reconstruction typically employed for CCTA25. The image noise level depends on the radiation dose; thus, an excessively low radiation dose may degrade image quality and ECV quantification. Although half-scan reconstruction (a technique where the scanner acquires data from just over 180° of rotation around the patient, rather than the full 360°, to create an image) is typically favored for its improved temporal resolution in CCTA, full-scan reconstruction may be more suitable for patients with stable heart rates, as it utilizes a sufficient radiation dose to enhance image quality.[25] Moreover, half-scan reconstruction inherently suffers from artifactual variations in CT numbers due to variations in beam hardening and scatter that depend on the X-ray source position.[26] The application of beam hardening correction can also be beneficial in refining image quality.[27] In dual-source CT, a hybrid reconstruction algorithm that integrates half-scan and full-scan technique has been shown to improve image quality and interobserver reproducibility compared with those of half-scan reconstruction (Fig. 1).[24] Currently, there is no consensus whether diastolic or systolic phase reconstruction is more appropriate for CT-LE imaging.

Multi-energy CT is a relatively recent advancement wherein attenuation data of different energies are acquired. It provides image sets such as iodine-specific images, virtual non-contrast images, effective atomic number images, and virtual mono-energetic images (VMI) (Fig. 2). VMI acquired at 40–50 keV contributes to better visual assessment of delayed enhancement in CT-LE and should be reconstructed.[28,29] Iodine-specific images improve the contrast-to-noise ratio and provide ECV without non-contrast data.[30] It has also been reported that dual-source photon counting detector (PCD) CT has enabled accurate quantification of ECV from the iodine ratio of LE scans.[31]

For comprehensive image interpretation, high-quality reconstruction of left ventricular short- and long-axis images is essential. This necessitates the acquisition of axial images with a thin slice thickness, ideally 1–2 mm, which facilitates detailed multiplanar reformat. For visual interpretation, reconstructions may be viewed at a thickness of approximately 5–8 mm to optimize the balance between image detail and noise reduction.

2.2. Amount of contrast media

Myocardial infarcts with high contrast comparable with that of LGE-MRI were depicted in some early animal studies on the feasibility of CT-LE; however, large amounts of contrast agent, such as 1000–1500 mgI (iodine)/kg, which is equivalent to 250 mL of contrast agent for a 75 kg person, were used in these studies.[32,33] The amount of contrast required for CCTA is at most approximately 300 mgI/kg. Although it is possible to detect myocardial infarction using CT-LE with a low contrast dose, sensitivity is inevitably reduced for identifying subendocardial infarction and non-ischemic fibrosis (Fig. 3).

There is no consensus on the contrast dose required for CT-LE, and contrast doses used in clinical studies for CT-LE have varied from 300 to 700 mgI/kg.[34] Kurobe et al. reported a significant difference in the contrast agent dose per body weight between cases that were visually judged to have good and poor contrast between the left ventricular myocardium and the left ventricular cavity (median, 651 mgI/kg; interquartile range, 597–693 mgI/kg vs. median, 584; interquartile range, 571–619 mgI/kg; $p = 0.041$), and reported that a dose of $\geq$600 mgI/kg (100 mL of 370 mgI/mL contrast agent for a 60 kg patient) is recommended.[24] Overall, adequate lesion delineation depends on the imaging protocol, reconstruction method, and target lesion (myocardial infarction vs. non-ischemic fibrosis), and further studies are needed to optimize the dose of contrast agent. However, a contrast dosing optimized for CCTA may be sufficient for ECV quantification.[35]

2.3. Delay time after contrast administration for CT-LE

There is no established consensus on the optimal timing between contrast administration and CT-LE acquisition. Jacquier et al. reported

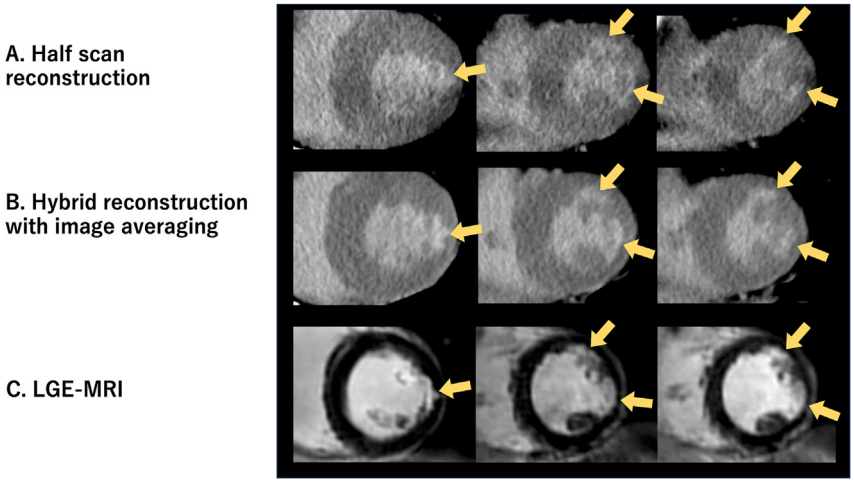

Fig. 1. Comparison of CT-LE imaging by conventional half-scan and hybrid reconstruction in a patient with no history of myocardial infarction. Subendocardial infarction in the lateral and anterior walls (arrows) were challenging to identify using half-scan reconstruction due to streaking artifacts (**A**). However, they were clearly visualized using hybrid reconstruction with image averaging (**B**), showing an excellent correlation with LGE- MRI (**C**). LGE, late gadolinium enhancement; MRI, magnetic resonance imaging; CT-LE, computed tomography late enhancement.

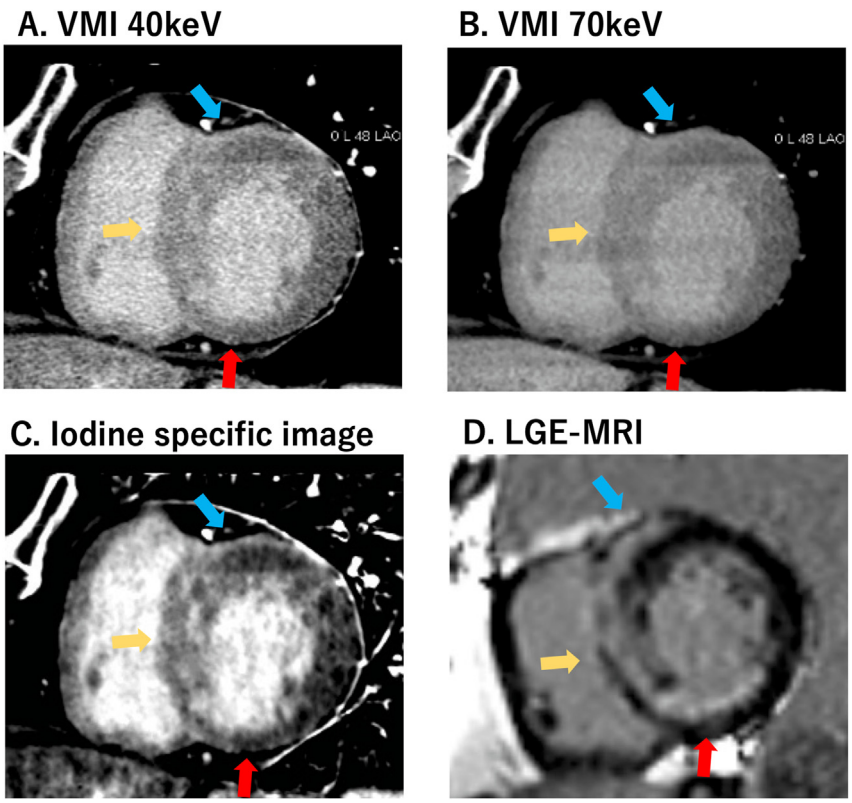

Fig. 2. CT-LE imaging with dual-energy CT in a patient with occluded right coronary artery and cardiac sarcoidosis. Myocardial CT-LE image shows subendocardial infarction in the inferior wall (red arrow), striated nonischemic enhancement (yellow arrow) in the mid-wall of the interventricular septum, and non-ischemic enhancement (blue arrow) in the epicardium of the anterior wall. The contrast of the lesion is higher in the VMI of 40 keV(**A**) and the iodine-specific images (**C**) compared with that of the 70 keV image (**B**). These lesions are in good agreement with LGE-MRI (**D**). CT-LE, computed tomography late enhancement; CT, computed tomography; VMI, virtual mono-energetic image. (For interpretation of the references to colour in this figure legend, the reader is referred to the Web version of this article.)

that contrast-enhanced CT performed 5 min after injection in patients with reperfused acute myocardial infarction yielded a higher signal-to-noise ratio and better image quality than those obtained at 10 min with no significant difference in the measured extent of infarction.[36] Similarly, Brodoefel et al., using a reperfused porcine model, compared delay times of 3, 5, 10, and 15 min and found that the contrast between viable and non-viable myocardium was the greatest at 3 and 5 min when using the bolus infusion protocol.[37] Hamdy et al. extended these findings to patients with old myocardial infarction, reporting that the best image quality was achieved at 5 min.[38] These studies collectively suggest a shorter delay time range of 3–10 min, shorter than the delay of over 10 min recommended for LGE-MRI. This shorter delay time strategy, aimed at improving signal-to-noise ratio, is presented as a countermeasure for insufficient contrast volume according to the standardized CMR protocol 2020 update.[39]

2.4. Radiation dose

The risk of radiation exposure should be carefully weighed against the benefit so that "as low as reasonably achievable (ALARA principle)"[40] for all patients, particularly for pregnant women, young patients, and children who require repeated examinations, while maintaining diagnostic image quality.

2.4.1. Single-energy approach

Radiation dose reduction in CT-LE in the single-energy approach can be achieved in a similar way to the reduction of exposure in CCTA. It is important to appropriately combine low tube potential scans, prospectively electrocardiography-triggered scans, and iterative reconstruction. CT-LE can be performed at 1–2 mSv.[12,41,42] However, it is necessary to consider radiation from the non-contrast scan to calculate ECV; thus,

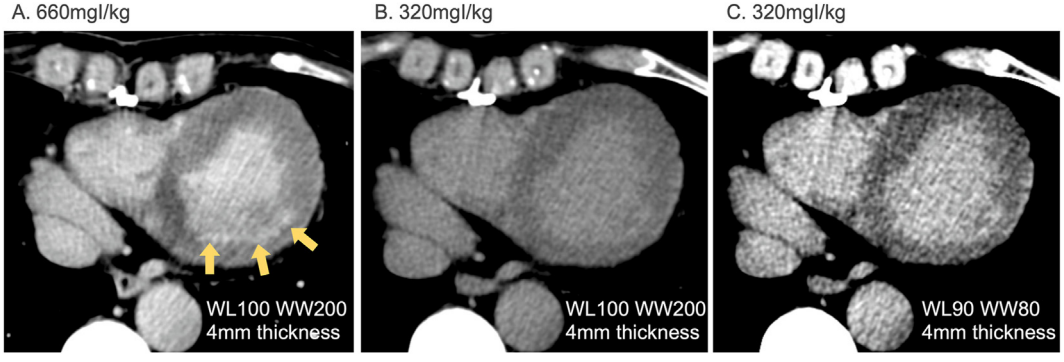

Fig. 3. CT-LE imaging obtained with 660 mgI/kg (**A**) and 320 mgI/kg (**B, C**) of iodine-based contrast medium in patient with a history of myocardial infarction. Subendocardial infarction is clearly visualized in the lateral wall with 660 mgI/kg (**A**), but is difficult to discern with 320 mgI/kg at the same window setting (B) or with a narrowed window setting (C). CT-LE, computed tomography late enhancement.

studies on CT-LE with ECV measurements have reported doses ranging between 3.1 and 5.8 mSv.[35,41,43,44]

2.4.2. Multi-energy approach

The tube current is adjustable in the multi-energy approach; however, the tube voltage is fixed for each device, and the options for the imager to reduce exposure are limited. In addition, depending on the CT platform, only retrospectively electrocardiography-gated helical scans may be available for cardiac scans. Thus, the low dose levels achieved through the single-energy approach for CCTA may be difficult to achieve through dual-energy acquisition. Radiation doses of GE, Philips, and Siemens scanners for dual-energy CT-LE have been reported as 2.2–3.6 mSv,[34,45] 2.5–4.8 mSv,[10,29] and 3.6–6.8 mSv,[46–48] respectively. Recent reports indicate that PCD-CT allows LE imaging at only 1.2–2 mSv.[31,49] Thus, the clinical use of CT-LE may expand with the spread of PCD-CT.

2.5. Qualitative and quantitative evaluation of CT-LE

LE images are usually evaluated qualitatively. It is useful to align the left ventricular short-axis images of the non-contrast-enhanced, CCTA, and LE images together when observing the images with an image viewer (Fig. 4). When observing LE images, it is appropriate to use a narrow window setting to emphasize the contrast. Moreover, the window settings should be adjusted appropriately depending on the tube voltage and VMI energy levels used. For example, when using a tube voltage of 120 kV, use a window level of 60–80 HU and a window width of 80–110 HU. Additionally, when adjusting window settings, consideration should also be given to CT scanner characteristics and image quality levels. The left ventricular inferior wall is susceptible to streak artifacts originating from the diaphragm; therefore, care should be taken when interpreting images.

Using LGE-MRI as a reference standard, Ohta et al. reported a sensitivity of 94.3 % and 97.1 % and a specificity of 88.9 % and 88.9 % for the diagnostic performance of 40 keV VMI and iodine-specific images in the detection of LE.[28] Oda et al. demonstrated that the interobserver agreement of VMI at 50 keV for the visual detection of LE was excellent and that the κ value (κ, 0.87) was higher than that for the standard 120 kV (κ, 0.70) and iodine-specific images (κ, 0.83). The agreement of VMI at 50 keV (κ, 0.90) and iodine-specific image (κ, 0.87) with LGE-MRI for detecting LE lesions was excellent; moreover, it was superior to that of standard 120-kV imaging (κ, 0.66).[29] The extent of LE legions can be computed in absolute parameters and expressed as the percentage of total left ventricular mass according to the following equations:[50]

LE volume (mL) = ΣLE area x slice thickness

LE mass (g) = ΣLE area x slice thickness x 1.06

LE extent (%) = LE mass (g)/LV mass (g) x 100

Recently, quantitative analysis of LE imaging has become feasible through the use of dedicated commercially available software.[9] Such software can facilitate an objective assessment of LE by automatically delineating myocardium exhibiting a CT number above a specified threshold (e.g. ≥5 standard deviations above the mean for CT number of remote myocardium) and quantifying the extent of LE as a percentage of total left ventricular area.

3. What is ECV? How to measure ECV by CT?

3.1. Principles and calculation of myocardial ECV

Myocardial fibrosis is a key pathologic condition in cardiomyopathies that is characterized by the excessive deposition of collagen-rich extracellular matrix proteins in the interstitial space of the myocardium, resulting in the expansion of the extracellular matrix structure. Although recent histological data have suggested overlap in conditions,[51] myocardial fibrosis has traditionally been categorized into interstitial fibrosis and replacement fibrosis. Detection of replacement fibrosis using LGE-MRI is a well-established technique. Moreover, cardiac MRI enables the non-invasive assessment of interstitial fibrosis with the quantification of myocardial T1 or ECV.[51–53] Myocardial ECV is a measure of the volume of the extracellular space, that is, the interstitial fluid or fibrosis-filled space surrounding myocardial cells in tissues. It is defined as the volume fraction of extra-cellular space and is expressed as shown below:

$$ECV = (1 - Ht) \cdot \lambda$$

where λ is the tissue-blood partition coefficient of the contrast medium in the myocardium, and *Ht* represents the blood hematocrit, which represents the proportion of the total blood volume that comprises red blood cells. Myocardial ECV with MRI represents the equilibrium distribution of gadolinium-based contrast material between the myocardium and blood and is derived from T1 measurements. λ is calculated using the pre- and post-contrast blood and myocardial T1 values as shown below:

$$\lambda = \frac{\Delta R1_M}{\Delta R1_B} = \frac{\frac{1}{T1_{Post\ M}} - \frac{1}{T1_{Pre\ M}}}{\frac{1}{T1_{Post\ B}} - \frac{1}{T1_{Pre\ B}}}$$

where ΔR1 is $1/T1_{Post} - 1/T1_{Pre}$ for the blood or myocardium, *Post* represents postcontrast, *Pre* represents precontrast, *M* represents myocardium, and *B* represents blood. This concept is now applied to iodine-contrast medium using cardiac CT. The λ for CT-ECV is calculated using the following equation:

$$\lambda = \frac{\Delta HU_M}{\Delta HU_B}$$

where ΔHU is the change in CT number.[41]

Han et al. demonstrated excellent correlation and small systemic bias in ECV quantification between MRI and CT (correlation, 0.90; 95 % CI, 0.86–0.95; bias, 0.96, 95 % CI, 0.14–1.78).[17] Zhang et al.

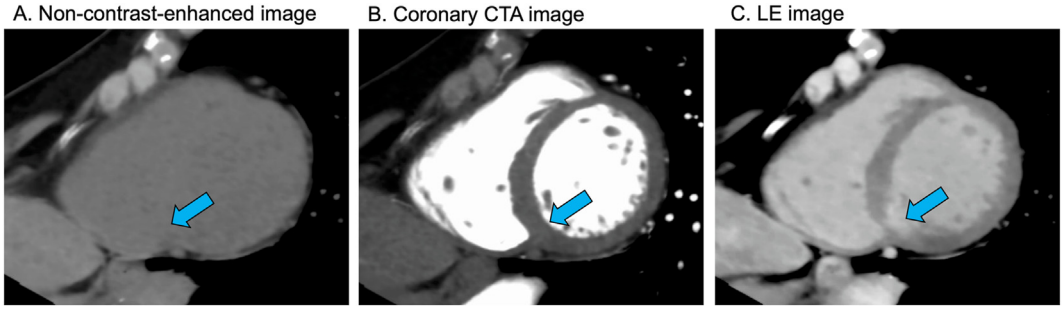

Fig. 4. Recommended visual observation method for LE images. When observing with an image viewer, it is useful to align the left ventricular short-axis images of non-contrast-enhanced (**A**), CCTA (**B**), and LE (**C**) images together. The extent of LE lesion (arrows) can be evaluated by comparing LE images and CCTA images. Non-contrast-enhanced images can confirm that the LE lesion is not calcification. LE, late enhancement; CCTA, coronary computed tomography angiography.

reported that the excellent correlation was consistent for both patient-based (correlation, 0.89 [95 % CI, 0.86–0.91]; bias, 0.07 [95 % CI, −0.42, 0.55]) and segment-based (correlation, 0.84 [95 % CI, 0.82–0.85]; bias, 0.44 [95 % CI, 0.16–0.72]) analyses.[54] However, Han et al. also reported that the results showed significant heterogeneity (I^2: 64 % for correlation and 89 % for bias, respectively; $p < 0.01$ for both)[17] and that the publication year was a significant source of heterogeneity in correlation. Specifically, the correlation between MRI-ECV and CT-ECV improved in more contemporary studies. This may reflect improvements in image quality and reduction of artifacts owing to advances in CT scanner and reconstruction software.

3.2. Methodology in ECV calculation using CT: subtraction and iodine-specific images

Two approaches are proposed to calculate CT-ECV: subtraction and iodine-specific images.[41,46] In the subtraction method, ECV is calculated from the aforementioned change in CT number between non-contrast and LE images. Iodine-specific images can be generated using a multi-energy CT without non-contrast CT. Compared with the subtraction method, multi-energy CT does not have the risk of misregistration. Moreover, it does not require a coregistration software. However, the subtraction method is available with all CT scanners even without dual energy CT capabilities. It is usually sufficient to quantify the ECV of intraventricular septum where most reliable quantification is possible (Fig. 5).

In a recent meta-analysis, Han et al. showed that the pooled correlation of studies that utilized iodine-specific images for ECV quantification was significantly higher than the pooled correlation of studies using the subtraction method (0.94 [95 % CI: 0.91–0.98] vs. 0.87 [95 % CI: 0.80–0.94], respectively, p for difference = 0.01).[17] No significant difference was observed in the pooled bias between studies using the subtraction method and those using iodine-specific images (1.00 % [95 % CI:0.58–2.58]) vs 0.85 % [95 % CI: 0.25%–1.95 %]; p for difference = 0.85). Zhang et al. also demonstrated in their meta-analysis that the correlation between CT and MRI of iodine-specific images (0.94 [95 % CI, 0.91–0.96]) was significantly higher than that of the subtraction method (0.84 [95 % CI: 0.80–0.88], $p = 0.03$), with no significant difference observed in the systemic bias (subtraction method (−0.72 % [95 % CI, −1.78%–0.35 %]) vs. iodine-specific images (0.67 % [95 % CI, 0.42%–0.92 %], $p = 0.21$)).[54]

3.3. Delay time after contrast administration for CT-ECV

Jablonowski et al. performed imaging at 1, 3, 5, and 10 min in an animal model of myocardial infarction and demonstrated that the measured ECV is stable from 3 min or later, except at the center of large infarcts.[55] Their experimental results are consistent with the simulation results of Jerosch-Herold et al., who showed that equilibrium can be reached at 4 min or later after contrast injection, except in tissue with extremely low perfusion.[56] Treibel et al. performed imaging at 5 and 15 min after bolus injection in patients with amyloidosis and those with severe aortic stenosis and reported that a delay time of 5 min was superior to 15 min in terms of signal-to-noise ratio, correlation with MRI, and correlation with clinical parameters known for tracking cardiac disease.[57] Hamdy et al. compared delay times of 3, 5, and 7 min after contrast administration and reported that ECV was stable regardless of the time point selected.[38] These studies collectively suggest that a delay time as short as 3 min may be sufficient for accurate and stable ECV measurement.

4. Advantages of CT-LE compared to LGE-MRI

In Table 1, we present a technical comparison between CT-LE and LGE-MRI.

LGE-MRI, acknowledged as the gold standard for evaluation of myocardial scar and fibrosis, holds Class I indications in many cardiomyopathy guidelines,[5,58] reflecting its widespread use and robust supporting evidence. In contrast, CT-LE has only been given a Class IIa indication for as an alternative to MRI in cardiac amyloidosis guidline.[59] Although LGE-MRI remains the preferred method for assessing cardiomyopathy, CT-LE emerges as a viable alternative to MRI, particularly in patients with non-MRI-compatible external devices, such as metallic implants, implantable electronic devices, and infusion pumps (Fig. 6).

In specific clinical scenarios, the additional acquisition of CT-LE underscores its utility. While CT is essential for preprocedural planning in transcatheter aortic valve replacement (TAVR), incorporating ECV measurement by CT could contribute to a comprehensive evaluation of underlying myocardial pathology, especially given that 16 % of patients with aortic stenosis may have transthyretin cardiac amyloidosis.[60] ECV quantification before TAVR proves useful for detecting underlying transthyretin cardiac amyloidosis and predicting patient prognosis.[61] CT excels in the 'triple rule-out' strategy for evaluating coronary artery disease, pulmonary embolism, and aortic dissection. In cases of

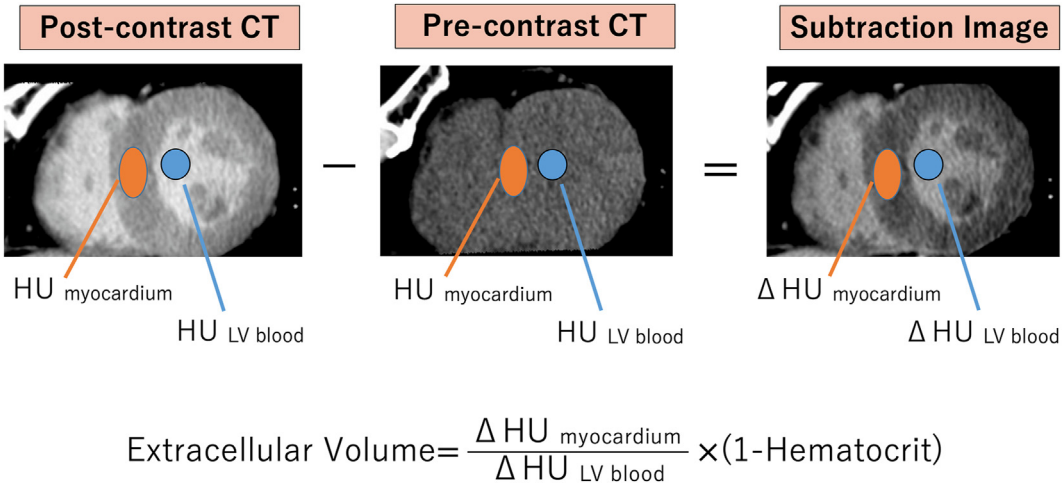

Fig. 5. Calculation of ECV in subtraction method. Regional ECV can be calculated by measuring the mean CT number in HU within a manually placed ROI on both LV blood and myocardium. Nevertheless, using the coregistration function of 3D workstations to generate a subtraction image may prove beneficial. This approach is advantageous because achieving precise alignment of ROIs on post-contrast and pre-contrast images is not always a straightforward process. ECV, extracellular volume; HU, Hounsfield unit; ROI, region of interest; LV, left ventricle.

Table 1
Pros and cons of myocardial CT late enhancement compared with LGE-MRI.

	CT		MRI	
Scan duration	◎	Single breath hold	○	Multiple breath holdings required depending on the number of imaging planes
Spatial resolution	◎	Iso-voxel, sub-millimeter resolution Possible for arbitrary planes	○	Limited through-plane resolution (6–8 mm), in-plane resolution (1.4–1.8 mm)
Contrast to noise ratio	○	Dependent on the tube potential (single-energy), x-ray energy of virtual monochromatic image or iodine specific image (multi-energy), or amount of contrast medium	◎	Adjustment of inversion time to null the normal myocardium
Extracellular volume fraction	○	Calculate from late enhancement image (subtraction or iodine specific image)	◎	Need of T1 mapping, one breath-hold per slice
Radiation exposure	△	Effort to dose reduction	◎	None
Devices with magnetic materials	○	Not contraindicated*	△	Contraindicated or conditional

Note. — ◎: excellent, ○: good, △: fair. * metal artifact+.

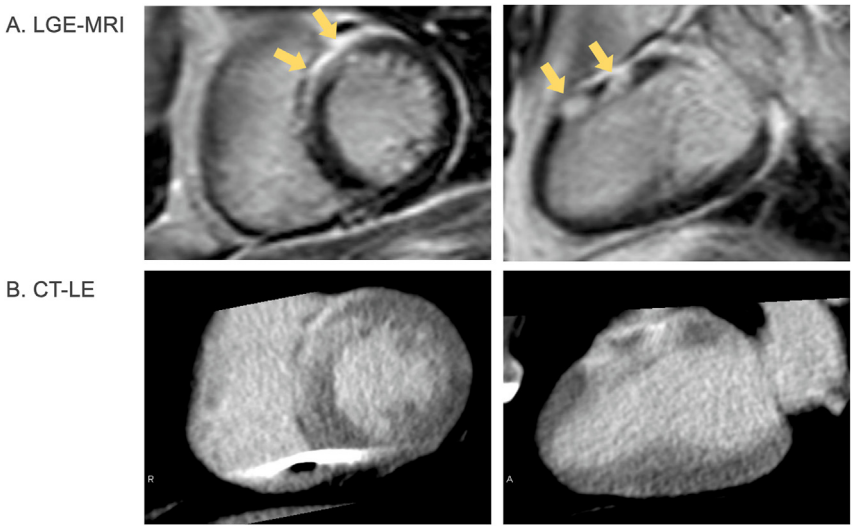

Fig. 6. LE in a patient with cardiac sarcoidosis assessed using (**A**) LGE-MRI before pacemaker placement, and (**B**) CT-LE after placement. Epicardial LE was revealed in the anteroseptal wall on LGE-MRI, and this finding is also well visualized by CT-LE despite the presence of metal artifact from the pacemaker leads in the inferior wall. LGE, late gadolinium enhancement; MRI, magnetic resonance imaging; CT-LE, computed tomography late enhancement; LE, late enhancement; CT, computed tomography.

troponin-positive acute chest pain, additional CT-LE and ECV measurements could be used for exclusion of myocarditis and myocardial infarction with non-obstructive coronary arteries (MINOCA).[62] Furthermore, CT is the first-line test in the assessment of chronic coronary syndrome.[63] The additional CT-LE can reveal unrecognized myocardial infarction, serving as an independent prognostic factor beyond the presence of obstructive coronary artery stenosis and the presence of ischemia.[64]

5. CT-LE with PCD-CT

PCD-CT is a cutting-edge technology that has sparked ongoing advancements and breakthroughs in diagnostic imaging. Traditional energy-integrating detector CT gauges the overall energy of x-rays by converting photons into visible light and subsequently employing photodiodes to convert visible light into digital signals. In contrast, PCD-CT directly records x-ray photons as electrical signals, bypassing the intermediate conversion to visible light. PCD-CT systems offer a range of advantages, including enhanced spatial resolution achieved through smaller detector pixels.[65–68] PCD-CT also heightened iodine image contrast, improved geometric dose efficiency enabled high-resolution imaging, reduced radiation exposure for all body parts, including cardiovascular lesions, multi-energy imaging capabilities, and diminished artifacts.

PCD-CT can also improve the visualization of abnormal enhancement in LE images via these characteristics (Fig. 7). Accurate quantification of

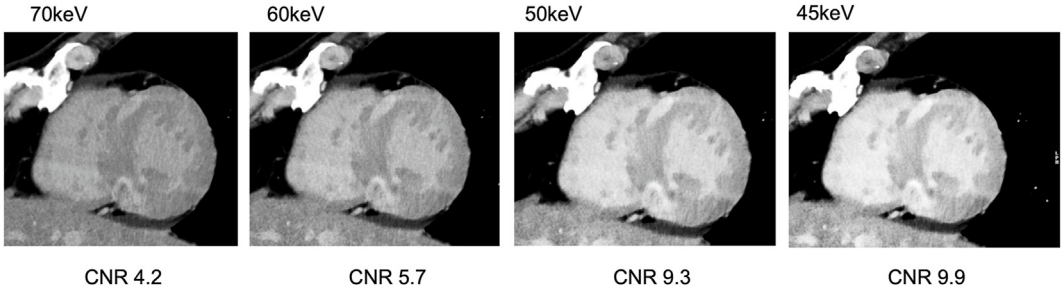

Fig. 7. LE in a patient with hypertrophic cardiomyopathy obtained with a dual-source photon-counting detector CT. Abnormal LE was observed at the right ventricular-left ventricular junction. Even in the lower monochromatic energy range, there is an improvement in contrast-to-noise ratio due to increased iodine contrast effect without an increase in noise. LE, late enhancement; CT, computed tomography; CNR, contrast-to-noise ratio.

ECV can be achieved by harnessing the capabilities of dual-source PCD-CT. The capability to characterize myocardial tissue using PCD-CT was emphasized in an in vivo study by Mergen et al.[31] PCD-CT virtual mono-energetic- and dual-energy-derived ECV quantification showed high correlation ($r = 0.87$, $p < 0.001$), with narrow limits of agreements and a mean error of 0.9 %. Aquino et al.[49] reported that the radiation dose for dual-energy PCD-CT was 40 % lower than that of single-energy PCD-CT (volume CT dose index, 10.1 mGy vs. 16.8 mGy). Compared with MRI, dual-energy PCD-CT showed a strong correlation ($r = 0.82$ and 0.91, both $p < 0.001$) and good to excellent reliability (intraclass correlation coefficients, 0.81 and 0.90) for midventricular and global ECV quantification.[49]

With enhanced material discrimination and reduced radiation exposure, which is expected to be achieved with advancements in CT equipment (e.g., PCD-CT), CT-LE may accumulate more robust evidence in the future.

6. Conclusion

CT-LE provides high diagnostic accuracy for late enhancement patterns in ischemic and non-ischemic cardiomyopathies. CT-LE offers superior spatial and temporal resolution compared with that of LGE-MRI. In addition, CT-derived ECV demonstrates a strong correlation with MRI-derived ECV. However, it is worth noting that the contrast-to-noise ratio of CT-LE is generally lower than that of LGE-MRI, and the quality of CT-LE is influenced by various factors, such as tube voltage, contrast media volume, reconstruction method, and acquisition timing after contrast injection. Therefore, it is crucial to perform CT-LE with a customized and optimized protocol tailored to each CT platform to achieve high-quality CT-LE while maintaining an appropriate radiation dose. The integration of PCD-CT technology will enhance the clinical usability of CT-LE by improving the overall image quality and reducing radiation exposure. This advancement positions CT-LE as a promising tool for characterizing myocardial pathologies.

Funding

None.

Data availability statement

Not applicable.

Declaration of competing interest

No author declared a conflict of interest with respect to this manuscript.

Other potentially competing interests were provided in detail separately.

Acknowledgements

We appreciate the support of working group of the Japanese Society of Advanced Computed Tomography.

We also wish to acknowledge Mr. Yu Ishizaka, RT for his contribution to the image creation for this article.

We would like to thank Editage (www.editage.jp) for English language editing.

References

1. Wesbey GE, Higgins CB, McNamara MT, et al. Effect of gadolinium-DTPA on the magnetic relaxation times of normal and infarcted myocardium. *Radiology*. 1984; 153(1):165–169.
2. Kim RJ, Wu E, Rafael A, et al. The use of contrast-enhanced magnetic resonance imaging to identify reversible myocardial dysfunction. *N Engl J Med*. 2000;343(20): 1445–1453.
3. Mahrholdt H, Wagner A, Judd RM, Sechtem U, Kim RJ. Delayed enhancement cardiovascular magnetic resonance assessment of non-ischaemic cardiomyopathies. *Eur Heart J*. 2005;26(15):1461–1474.
4. Di Marco A, Brown P, Mateus G, et al. Late gadolinium enhancement and the risk of ventricular arrhythmias and sudden death in NYHA class I patients with non-ischaemic cardiomyopathy. *Eur J Heart Fail*. 2023;25(5):740–750.
5. Arbelo E, Protonotarios A, Gimeno JR, et al. 2023 ESC Guidelines for the management of cardiomyopathies. *Eur Heart J*. 2023;44(37):3503–3626.
6. Higgins CB, Siemers PT, Newell JD, Schmidt W. Role of iodinated contrast material in the evaluation of myocardial infarction by computerized transmission tomography. *Invest Radiol*. 1980;15(6 Suppl):S176–S182.
7. Rodriguez-Granillo GA, Rosales MA, Baum S, et al. Early assessment of myocardial viability by the use of delayed enhancement computed tomography after primary percutaneous coronary intervention. *JACC Cardiovasc Imaging*. 2009;2(9): 1072–1081.
8. Shiozaki AA, Senra T, Arteaga E, et al. Myocardial fibrosis detected by cardiac CT predicts ventricular fibrillation/ventricular tachycardia events in patients with hypertrophic cardiomyopathy. *J Cardiovasc Comput Tomogr*. 2013;7(3):173–181.
9. Aikawa T, Oyama-Manabe N, Naya M, et al. Delayed contrast-enhanced computed tomography in patients with known or suspected cardiac sarcoidosis: a feasibility study. *Eur Radiol*. 2017;27(10):4054–4063.
10. Kidoh M, Oda S, Takashio S, et al. CT extracellular volume fraction versus myocardium-to-lumen signal ratio for cardiac amyloidosis. *Radiology*. 2022:220542. Published online October 18.
11. Scully PR, Bastarrika G, Moon JC, Treibel TA. Myocardial extracellular volume quantification by cardiovascular magnetic resonance and computed tomography. *Curr Cardiol Rep*. 2018;20(3):15.
12. Andreini D, Conte E, Mushtaq S, et al. Comprehensive evaluation of left ventricle dysfunction by a new computed tomography scanner: the E-PLURIBUS study. *JACC Cardiovasc Imaging*. 2022. https://doi.org/10.1016/j.jcmg.2022.08.005. Published online October 19.
13. Mukai-Yatagai N, Ohta Y, Amisaki R, et al. Myocardial delayed enhancement on dual-energy computed tomography: the prevalence and related factors in patients with suspicion of coronary artery disease. *J Cardiol*. 2020;75(3):302–308.
14. Goto Y, Kitagawa K, Nakamura S, et al. Prognostic value of cardiac CT delayed enhancement imaging in patients with suspected coronary artery disease. *JACC Cardiovasc Imaging*. 2021;14(8):1674–1675.
15. Sado DM, Flett AS, Banypersad SM, et al. Cardiovascular magnetic resonance measurement of myocardial extracellular volume in health and disease. *Heart*. 2012; 98(19):1436–1441.
16. Tham EB, Haykowsky MJ, Chow K, et al. Diffuse myocardial fibrosis by T1-mapping in children with subclinical anthracycline cardiotoxicity: relationship to exercise capacity, cumulative dose and remodeling. *J Cardiovasc Magn Reson*. 2013;15(1):48.
17. Han D, Lin A, Kuronuma K, et al. Cardiac computed tomography for quantification of myocardial extracellular volume fraction. *JACC Cardiovasc Imaging*. 2023;16(10): 1306–1317.
18. Koweek L, Achenbach S, Berman DS, et al. Standardized medical terminology for cardiac computed tomography 2023 update: an expert consensus document of the society of cardiovascular computed tomography (SCCT), American association of physicists in medicine (AAPM), American college of radiology (ACR), North American society for cardiovascular imaging (NASCI) and radiological society of North America (RSNA) and endorsement by the Asian society of cardiovascular imaging and the European society of cardiovascular radiology. *J Cardiovasc Comput Tomogr*. 2023;17(5):345–354.
19. Nieman K, Shapiro MD, Ferencik M, et al. Reperfused myocardial infarction: contrast-enhanced 64-Section CT in comparison to MR imaging. *Radiology*. 2008; 247(1):49–56.
20. Kishimoto J, Ohta Y, Kitao S, Watanabe T, Ogawa T. Image quality improvements using adaptive statistical iterative reconstruction for evaluating chronic myocardial infarction using iodine density images with spectral CT. *Int J Cardiovasc Imag*. 2018; 34(4):633–639.
21. Tanabe Y, Kido T, Kurata A, et al. Impact of knowledge-based iterative model reconstruction on myocardial late iodine enhancement in computed tomography and comparison with cardiac magnetic resonance. *Int J Cardiovasc Imag*. 2017;33(10): 1609–1618.
22. Takaoka H, Funabashi N, Ozawa K, et al. Improved diagnosis of detection of late enhancement in left ventricular myocardium using 2nd generation 320-slice CT reconstructed with FIRST in non-ischemic cardiomyopathy. *Int Heart J*. 2018;59(3): 542–549.
23. Takafuji M, Kitagawa K, Mizutani S, et al. Deep-learning reconstruction to improve image quality of myocardial dynamic CT perfusion: comparison with hybrid iterative reconstruction. *Clin Radiol*. 2022;77(10):e771–e775.
24. Kurobe Y, Kitagawa K, Ito T, et al. Myocardial delayed enhancement with dual-source CT: advantages of targeted spatial frequency filtration and image averaging over half-scan reconstruction. *J Cardiovasc Comput Tomogr*. 2014;8(4):289–298.
25. Funama Y, Oda S, Kidoh M, Sakabe D, Nakaura T. Effect of image quality on myocardial extracellular volume quantification using cardiac computed tomography: a Phantom study. *Acta Radiol*. 2022;63(2):159–165.
26. Ramirez-Giraldo JC, Yu L, Kantor B, Ritman EL, McCollough CH. A strategy to decrease partial scan reconstruction artifacts in myocardial perfusion CT: phantom and in vivo evaluation. *Med Phys*. 2012;39(1):214–223.
27. Emoto T, Kidoh M, Oda S, et al. Myocardial extracellular volume quantification in cardiac CT: comparison of the effects of two different iterative reconstruction algorithms with MRI as a reference standard. *Eur Radiol*. 2020;30(2):691–701.
28. Ohta Y, Kitao S, Yunaga H, et al. Myocardial delayed enhancement CT for the evaluation of heart failure: comparison to MRI. *Radiology*. 2018;288(3):682–691.

29. Oda S, Emoto T, Nakaura T, et al. Myocardial late iodine enhancement and extracellular volume quantification with dual-layer spectral detector dual-energy cardiac CT. *Radiology: Cardiothoracic Imaging*. 2019;1(1):e180003, 04/.
30. Kalisz K, Halliburton S, Abbara S, et al. Update on cardiovascular applications of multienergy CT. *Radiographics*. 2017;37(7):1955–1974.
31. Mergen V, Sartoretti T, Klotz E, et al. Extracellular volume quantification with cardiac late enhancement scanning using dual-source photon-counting detector CT. *Invest Radiol*. 2022;57(6):406–411.
32. Baks T, Cademartiri F, Moelker AD, et al. Multislice computed tomography and magnetic resonance imaging for the assessment of reperfused acute myocardial infarction. *J Am Coll Cardiol*. 2006;48(1):144–152.
33. Lardo AC, Cordeiro MAS, Silva C, et al. Contrast-enhanced multidetector computed tomography viability imaging after myocardial infarction: characterization of myocyte death, microvascular obstruction, and chronic scar. *Circulation*. 2006; 113(3):394–404.
34. Rodriguez-Granillo GA. Delayed enhancement cardiac computed tomography for the assessment of myocardial infarction: from bench to bedside. *Cardiovasc Diagn Ther*. 2017;7(2):159–170.
35. Takafuji M, Kitagawa K, Nakamura S, et al. Feasibility of extracellular volume fraction calculation using myocardial CT delayed enhancement with low contrast media administration. *J Cardiovasc Comput Tomogr*. 2020;14(6): 524–528, 11.
36. Jacquier A, Boussel L, Amabile N, et al. Multidetector computed tomography in reperfused acute myocardial infarction. Assessment of infarct size and no-reflow in comparison with cardiac magnetic resonance imaging. *Invest Radiol*. 2008;43(11): 773–781.
37. Brodoefel H, Reimann A, Klumpp B, et al. Assessment of myocardial viability in a reperfused porcine model: evaluation of different MSCT contrast protocols in acute and subacute infarct stages in comparison with MRI. *J Comput Assist Tomogr*. 2007; 31(2):290–298.
38. Hamdy A, Kitagawa K, Goto Y, et al. Comparison of the different imaging time points in delayed phase cardiac CT for myocardial scar assessment and extracellular volume fraction estimation in patients with old myocardial infarction. *Int J Cardiovasc Imag*. 2019;35(5):917–926, 5.
39. Kramer CM, Barkhausen J, Bucciarelli-Ducci C, Flamm SD, Kim RJ, Nagel E. Standardized cardiovascular magnetic resonance imaging (CMR) protocols: 2020 update. *J Cardiovasc Magn Reson*. 2020;22(1):17, 12.
40. Prasad KN, Cole WC, Haase GM. Radiation protection in humans: extending the concept of as low as reasonably achievable (ALARA) from dose to biological damage. *Br J Radiol*. 2004;77(914):97–99.
41. Nacif MS, Kawel N, Lee JJ, et al. Interstitial myocardial fibrosis assessed as extracellular volume fraction with low-radiation-dose cardiac CT. *Radiology*. 2012; 264(3):876–883.
42. Bandula S, White SK, Flett AS, et al. Measurement of myocardial extracellular volume fraction by using equilibrium contrast-enhanced CT: validation against histologic findings. *Radiology*. 2013;269(2):396–403.
43. Scully PR, Patel KP, Saberwal B, et al. Identifying cardiac amyloid in aortic stenosis: ECV quantification by CT in TAVR patients. *JACC Cardiovasc Imaging*. 2020;13(10): 2177–2189.
44. Emoto T, Oda S, Kidoh M, et al. Myocardial extracellular volume quantification using cardiac computed tomography: a comparison of the dual-energy iodine method and the standard subtraction method. *Acad Radiol*. 2021;28(5):e119–e126.
45. Ohta Y, Kitao S, Yunaga H, et al. Quantitative evaluation of non-ischemic dilated cardiomyopathy by late iodine enhancement using rapid kV switching dual-energy computed tomography: a feasibility study. *J Cardiovasc Comput Tomogr*. 2019;13(2): 148–156, 03.
46. Lee HJ, Im DJ, Youn JC, et al. Myocardial extracellular volume fraction with dual-energy equilibrium contrast-enhanced cardiac CT in nonischemic cardiomyopathy: a prospective comparison with cardiac MR imaging. *Radiology*. 2016;280(1):49–57, 07.
47. Chang S, Han K, Youn JC, et al. Utility of dual-energy CT-based monochromatic imaging in the assessment of myocardial delayed enhancement in patients with cardiomyopathy. *Radiology*. 2018;287(2):442–451.
48. Abadia AF, van Assen M, Martin SS, et al. Myocardial extracellular volume fraction to differentiate healthy from cardiomyopathic myocardium using dual-source dual-energy CT. *J Cardiovasc Comput Tomogr*. 2020;14(2):162–167.
49. Aquino GJ, O'Doherty J, Schoepf UJ, et al. Myocardial characterization with extracellular volume mapping with a first-Generation photon-counting detector CT with MRI reference. *Radiology*. 2023;307(2):e222030.
50. Gerber BL, Belge B, Legros GJ, et al. Characterization of acute and chronic myocardial infarcts by multidetector computed tomography: comparison with contrast-enhanced magnetic resonance. *Circulation*. 2006;113(6):823–833.
51. Treibel TA, López B, González A, et al. Reappraising myocardial fibrosis in severe aortic stenosis: an invasive and non-invasive study in 133 patients. *Eur Heart J*. 2018; 39(8):699–709.
52. Nakamori S, Dohi K, Ishida M, et al. Native T1 mapping and extracellular volume mapping for the assessment of diffuse myocardial fibrosis in dilated cardiomyopathy. *JACC Cardiovasc Imaging*. 2018;11(1):48–59.
53. de Meester de Ravenstein C, Bouzin C, Lazam S, et al. Histological Validation of measurement of diffuse interstitial myocardial fibrosis by myocardial extravascular volume fraction from Modified Look-Locker imaging (MOLLI) T1 mapping at 3 T. *J Cardiovasc Magn Reson*. 2015;17(1):48.
54. Zhang H, Guo H, Liu G, et al. CT for the evaluation of myocardial extracellular volume with MRI as reference: a systematic review and meta-analysis. *Eur Radiol*. 2023;33(12):8464–8476.
55. Jablonowski R, Wilson MW, Do L, Hetts SW, Saeed M. Multidetector CT measurement of myocardial extracellular volume in acute patchy and contiguous infarction: validation with microscopic measurement. *Radiology*. 2015;274(2): 370–378.
56. Jerosch-Herold M, Sheridan DC, Kushner JD, et al. Cardiac magnetic resonance imaging of myocardial contrast uptake and blood flow in patients affected with idiopathic or familial dilated cardiomyopathy. *Am J Physiol Heart Circ Physiol*. 2008; 295(3):H1234–H1242.
57. Treibel TA, Bandula S, Fontana M, et al. Extracellular volume quantification by dynamic equilibrium cardiac computed tomography in cardiac amyloidosis. *J Cardiovasc Comput Tomogr*. 2015;9(6):585–592.
58. von Knobelsdorff-Brenkenhoff F, Schulz-Menger J. Cardiovascular magnetic resonance in the guidelines of the European Society of Cardiology: a comprehensive summary and update. *J Cardiovasc Magn Reson*. 2023;25(1):42.
59. Kitaoka H, Izumi C, Izumiya Y, et al. JCS 2020 guideline on diagnosis and treatment of cardiac amyloidosis. *Circ J*. 2020;84:1610–1671.
60. Castaño A, Narotsky DL, Hamid N, et al. Unveiling transthyretin cardiac amyloidosis and its predictors among elderly patients with severe aortic stenosis undergoing transcatheter aortic valve replacement. *Eur Heart J*. 2017;38(38):2879–2887.
61. Han D, Tamarappoo B, Klein E, et al. Computed tomography angiography-derived extracellular volume fraction predicts early recovery of left ventricular systolic function after transcatheter aortic valve replacement. *European Heart Journal - Cardiovascular Imaging*. 2021;22(2):179–185.
62. Palmisano A, Vignale D, Tadic M, et al. Myocardial late contrast enhancement CT in troponin-positive acute chest pain syndrome. *Radiology*. 2022;302(3):545–553.
63. Knuuti J, Wijns W, Saraste A, et al. 2019 ESC Guidelines for the diagnosis and management of chronic coronary syndromes. *Eur Heart J*. 2020;4:407–477.
64. Nakamura S, Kitagawa K, Goto Y, et al. Prognostic value of stress dynamic computed tomography perfusion with computed tomography delayed enhancement. *JACC Cardiovasc Imaging*. 2020;13:1721–1734.
65. Nehra AK, Rajendran K, Baffour FI, et al. Seeing more with less: clinical benefits of photon-counting detector CT. *Radiographics*. 2023;43(5):e220158.
66. Sawall S, Klein L, Amato C, et al. Iodine contrast-to-noise ratio improvement at unit dose and contrast media volume reduction in whole-body photon-counting CT. *Eur J Radiol*. 2020;126:108909.
67. Cademartiri F, Meloni A, Pistoia L, et al. Dual-source photon-counting computed tomography-Part I: clinical overview of cardiac CT and coronary CT angiography applications. *J Clin Med Res*. 2023;12(11):3627.
68. Mergen V, Eberhard M, Manka R, Euler A, Alkadhi H. First in-human quantitative plaque characterization with ultra-high resolution coronary photon-counting CT angiography. *Front Cardiovasc Med*. 2022;9:981012.